

Four level, atomic Cs laser at 852.1 nm with a quantum efficiency above 98%: Observation of three body photoassociation

J. D. Readle,^{1,a)} J. G. Eden,¹ J. T. Verdeyen,² and D. L. Carroll²

¹Laboratory for Optical Physics and Engineering, Department of Electrical and Computer Engineering, University of Illinois, Urbana, Illinois 61801, USA

²CU Aerospace, 2100 South Oak Street, Suite 206, Champaign, Illinois 61820, USA

(Received 24 March 2010; accepted 8 May 2010; published online 14 July 2010)

Lasing on the D_2 ($6p\ ^2P_{3/2} \rightarrow 6s\ ^2S_{1/2}$) transition of atomic Cs at 852.1 nm has been observed with a four level system in which the Cs $6p\ ^2P_{3/2}$ state is pumped by the photoassociation and subsequent dissociation of Cs-rare gas collision pairs. Characterized by a quantum efficiency $>98\%$, this laser requires no atomic precursor to the upper laser level and provides oscillation on an alkali transition inaccessible to three level, photopumped alkali laser systems. Measurements of photoabsorption and pump energy threshold in Cs–Ar–Kr mixtures reveal the influence of *three body* photoassociation. © 2010 American Institute of Physics. [doi:10.1063/1.3452338]

Quantum efficiency is one measure of the ultimate performance and utility of a laser. In this regard, the three level optically pumped alkali lasers (Cs, Rb, K) (Refs. 1–3) are distinctive in that direct photoexcitation of the lowest $np\ ^2P_{3/2}$ state ($n=4-6$ for K, Rb, and Cs, respectively) and subsequent lasing on the D_1 ($n\ ^2P_{1/2} \rightarrow n\ ^2S_{1/2}$) transition yield quantum efficiencies above 90%, limited only by the alkali $np\ ^2P_{3/2} - np\ ^2P_{1/2}$ fine structure splitting. Although this energy defect is sufficiently large in Cs, for example, to restrict the D_1 laser quantum efficiency to 95%, a greater drawback of the three level alkali system is the requirement for a relaxant species to collisionally transfer the $^2P_{3/2}$ population into the $^2P_{1/2}$ state without quenching, to a significant degree, the pumped $^2P_{3/2}$ level. Typically a hydrocarbon such as C_2H_6 , the relaxant presents long-term reliability and laser medium optical quality concerns owing to gradual pyrolysis of the relaxant which, in addition to the depletion of the molecule, results in the formation of alkali-hydride particulates and carbon deposits.

This letter reports the observation of lasing on the D_2 transition ($6p\ ^2P_{3/2} \rightarrow 6s\ ^2P_{1/2}$) of Cs at 852.1 nm when thermal Cs-rare gas (Ar, Kr) atomic collision pairs are photoassociated in a broad (~ 3 nm full width at half maximum) wavelength region centered at ~ 837 nm. Pumped by the dissociation of Cs-rare gas diatomic excimer molecules in the repulsive $B\ ^2\Sigma^+$ state, this four level laser has a quantum efficiency $>98\%$ because the lasing transition originates from the atomic state populated by the pump through Cs-rare gas molecular dissociation, terminates on ground, and the Cs-rare gas interaction is weak. It should be emphasized that lasing on the D_2 transition of the alkali atoms is not allowed with the three level atomic scheme employed previously.¹⁻³ Oscillation on the Cs D_2 transition demonstrates vividly that this Cs-rare gas laser system must be treated on a four level basis, despite the short lifetimes of the intermediate species (the alkali-rare gas complex) in its ground and excited states. Furthermore, the photoassociation of ternary Cs–Ar–Kr ensembles has been observed. Having an 852.1 nm laser excitation spectrum virtually identical to that for Cs–Ar pairs, the

photoassociation of Cs–Ar–Kr complexes lowers the pump energy threshold by $>25\%$.

In the semiclassical view, the photoassociation of Cs-rare gas pairs in the thermal continuum of the $X\ ^2\Sigma^+$ ground state interaction potential occurs predominantly in the region of internuclear separation in which the $B\ ^2\Sigma^+ - X\ ^2\Sigma^+$ difference potential varies slowly. Such free-free optical transitions of the binary Cs-rare gas complex define the blue satellite of the D_2 transition and provide a vehicle by which the atomic laser upper level can be accessed directly with a broadband optical source. Although a similar process sequence has proven successful in demonstrating lasing on the D_1 line of Cs (894.3 nm) in Cs–Ar– C_2H_6 and Cs–Kr– C_2H_6 mixtures,⁴⁻⁶ the experiments described here demonstrate that neither the Cs $6\ ^2P_{1/2}$ intermediate state nor an auxiliary species in the gas phase, such as the relaxant C_2H_6 , is necessary.

Pump/lasing cycles sharing several characteristics of the scheme described here have been reported previously. In 1979, Chilukuri⁷ observed super-radiance on the green $^2S_{1/2} \rightarrow ^2P_{3/2}$ transition (535.1 nm) of atomic thallium in Tl–Hg vapor mixtures when pumping several nm to the red of the 377.6 nm resonance transition. Subsequently, Atamas *et al.*⁸ photoexcited Tl 3.9 nm into the violet wing of the 377.6 nm line, pressure-broadened by He. In both sets of experiments, however, the lasing transition terminated on the $^2P_{1/2}$ metastable atomic state lying ~ 1 eV above ground.

The experimental arrangement and data acquisition procedures for these studies are similar to those described previously^{4,5} and will only be reviewed briefly here. A pulsed dye laser, tunable over the $\sim 819-865$ nm region and driven by the second harmonic of an Nd:YAG laser system, served as the optical pump source. After two stages of amplification, the pump pulses have an energy ≤ 2 mJ and a temporal width of ~ 4 ns. The optical cavity is an L-configuration that provides for two passes of the pump beam through the gain medium, and comprises a high reflector ($>97\%$ reflectivity at 852 nm) and a $\sim 50\%$ output coupler. Separated by ~ 80 cm, the mirrors have a radius of curvature of 3 m. Natural abundance Cs and either Ar at a number density of $\sim 1.6 \times 10^{19}$ cm⁻³ (500 Torr at room temperature) or an Ar/Kr mixture at the same total pressure were contained in a

^{a)}Electronic mail: jreadle@illinois.edu.

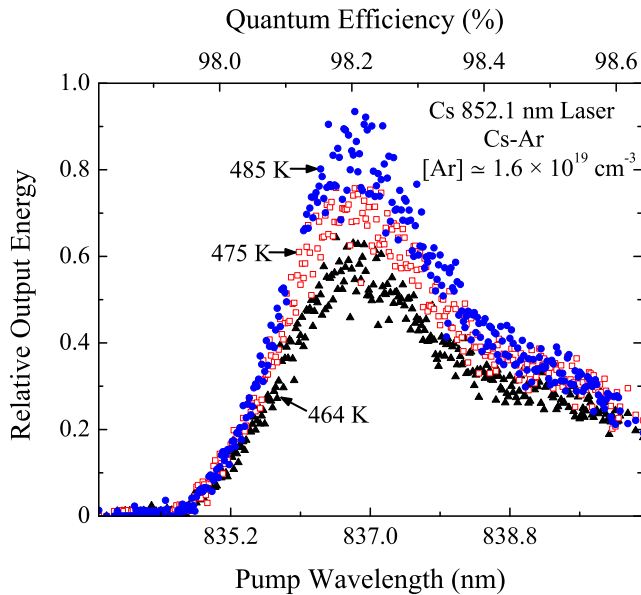


FIG. 1. (Color online) Excitation spectra recorded for Cs vapor-Ar mixtures by monitoring the 852.1 nm relative laser pulse energy as the pump dye laser wavelength (lower abscissa) was tuned over the ~ 834 – 840 nm region. The Ar number density was fixed at $\sim 1.6 \times 10^{19} \text{ cm}^{-3}$ and data were obtained for three temperatures [464 K (solid triangles: \blacktriangle), 475 K (open squares: \square), and 485 K (solid circles: \bullet)] which correspond to $[\text{Cs}] = 1.3 \times 10^{15} \text{ cm}^{-3}$, $1.9 \times 10^{15} \text{ cm}^{-3}$, and $2.8 \times 10^{15} \text{ cm}^{-3}$, respectively. The upper abscissa indicates the quantum efficiency of this D_2 laser for a given pump wavelength.

cylindrical optical cell, 2.5 cm in diameter and 10 cm in length, that was inserted into the resonator. The energies of the incident pump pulses, unabsorbed pump emerging from the resonator, and the output of the 852 nm Cs laser, were recorded with three calibrated pyroelectric detectors. For the alkali laser pulse energy measurements, scattered pump radiation was rejected by a bandpass filter having a transmittance of $45 \pm 5\%$ at 852 nm and a spectral width of ~ 8 nm. Tests revealed no detectable leakage through the filter when the pump laser wavelength $\lambda_p \leq 841$ nm.

Initial experiments were conducted with Cs–Ar mixtures ($[\text{Ar}] \approx 1.6 \times 10^{19} \text{ cm}^{-3}$) and Fig. 1 presents several excitation spectra acquired by recording the 852 nm laser pulse energy as λ_p was scanned over the 834–840 nm spectral interval. All of the data shown represent the average of four measurements. In order to account for pulse-to-pulse fluctuations in the pump energy, and the variation in dye laser output over this wavelength region, the energy of each Cs laser pulse was normalized to the incident pump energy. Data are given in Fig. 1 for optical cell temperatures of 464 K, 475 K, and 485 K, which correspond to Cs number densities of $[\text{Cs}] = 1.3 \times 10^{15} \text{ cm}^{-3}$, $1.9 \times 10^{15} \text{ cm}^{-3}$, and $2.8 \times 10^{15} \text{ cm}^{-3}$, respectively. As observed previously in Cs D_1 laser (894.3 nm) experiments with Cs–Ar– C_2H_6 mixtures,^{4,5} the peak of the Fig. 1 excitation spectrum at ~ 836.7 nm coincides with the position of the maximum of the D_2 line blue satellite in Cs–Ar mixtures.⁴ Furthermore, the breadth of the excitation spectrum is ≈ 3 nm at $[\text{Cs}] \sim 10^{15} \text{ cm}^{-3}$ but the spectral profile narrows slightly at higher alkali number densities, presumably owing to the increased temperature and the concomitant slight shift in the Franck–Condon region for the photoassociation process. The upper of the two abscissas of Fig. 1, which indicates the

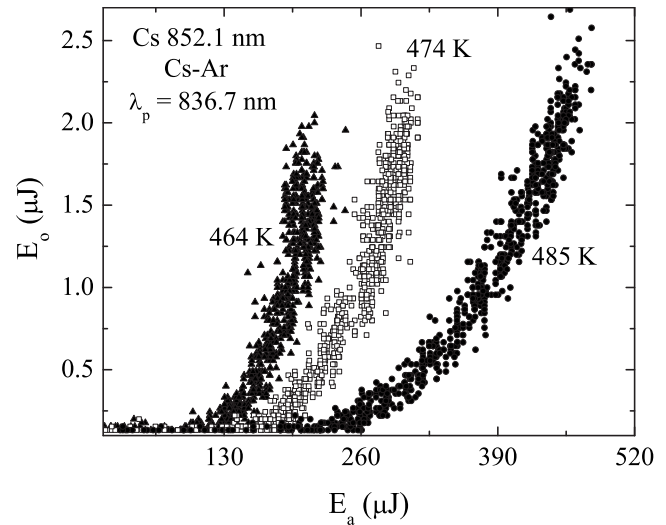


FIG. 2. Dependence of the 852.1 nm laser pulse energy (E_0) on the absorbed pump pulse energy (E_a) for a dye laser excitation wavelength (λ_p) of 836.7 nm. Argon is again the sole rare gas and $[\text{Ar}] \approx 1.6 \times 10^{19} \text{ cm}^{-3}$. The cell temperatures (and corresponding $[\text{Cs}]$ values) are the same as those for Fig. 1.

quantum efficiency (η) of the D_2 laser for a given pump wavelength, shows that $\eta > 98\%$ for all $\lambda_p > 835$ nm.

Measurements of the variation in the 852 nm laser pulse energy with the pump energy absorbed by the gain medium (E_a) are summarized in Fig. 2 for the same optical cell temperatures as those of Fig. 1. Note that the threshold absorbed pump pulse energy for $[\text{Cs}] = 1.3 \times 10^{15} \text{ cm}^{-3}$ (464 K) of $\sim 130 \mu\text{J}$ is quite close to the corresponding value recorded for the D_1 laser (894.3 nm) operating in Cs–Kr– C_2H_6 mixtures at a comparable temperature [$E_a(\text{threshold}) = 140 \mu\text{J}$ at 468 K]. This result is somewhat surprising because the degeneracy ($2J+1$) for the $6^2\text{P}_{3/2}$ upper laser level in the present experiments is twice that for the D_1 laser, thus suggesting a higher pump energy threshold for the 852.1 nm laser. Nevertheless, the threshold pump energies for the three sets of data in Fig. 2— $130 \mu\text{J}$, $175 \mu\text{J}$, and $250 \mu\text{J}$ for 464 K, 475 K, and 485 K, respectively—vary linearly with $[\text{Cs}]$ as one would expect. It is also evident that, for a fixed value of $[\text{Cs}]$, the slope efficiencies of Fig. 2 increase with E_a .

Unexpected behavior is observed when experiments identical to those described above were conducted with Cs–Ar–Kr mixtures in which $[\text{Ar}] = [\text{Kr}] = 8 \times 10^{18} \text{ cm}^{-3}$. Motivated by the recent observation⁶ that Cs–Kr pair absorption in the D_2 blue satellite peaks at ~ 841.1 nm, these experiments were directed to the synthesis of satellite photoabsorption spectra broader than those available with a single rare gas. Spectral engineering of the alkali-rare gas pump band by the superposition of binary alkali-rare gas absorption profiles might well lead to pump acceptance bandwidths > 5 – 6 nm. However, as illustrated in Fig. 3 for a constant $[\text{Cs}] = 1.3 \times 10^{15} \text{ cm}^{-3}$ (464 ± 2 K), the D_2 laser excitation spectrum for Cs–Ar–Kr mixtures (open circles: \circ) is indistinguishable from that for Cs–Ar (solid triangles: \blacktriangle). The maximum for both spectra lies at ~ 836.7 nm and the Cs–Kr peak⁶ at 841.1 nm is extremely weak. Further insight into the dynamics of the D_2 laser in multi-rare gas environments is provided by measurements of the 852 nm laser output energy. Panel (a) of Fig. 4 presents data acquired for both Cs–Ar and Cs–Ar–Kr mixtures at 464 ± 2 K. In obtaining

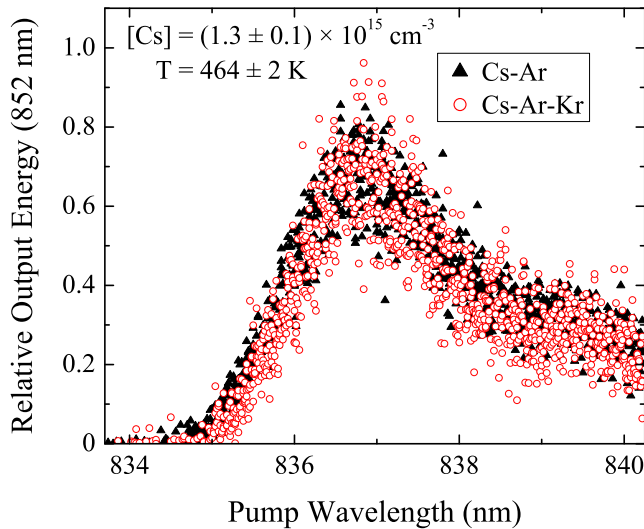


FIG. 3. (Color online) Comparison of the excitation spectral data of Fig. 1 (solid triangles: \blacktriangle) with similar measurements in Cs–Ar–Kr (open circles: \circ) mixtures for which $[\text{Ar}] = [\text{Kr}] = 8 \times 10^{18} \text{ cm}^{-3}$ (total rare gas pressure at 300 K of 500 Torr). The optical cell temperature for both sets of measurements was fixed at $464 \pm 2 \text{ K}$.

these results, the laser was photoexcited at 836.7 nm and the output pulse energy (E_o) was recorded for incident pulse energies up to $\sim 2.3 \text{ mJ}$. It is clear from Fig. 4(a) that the threshold pump pulse energy for the ternary Cs–Ar–Kr mixture is $\sim 600 \mu\text{J}$, or $\sim 28\%$ lower than that for Cs–Ar alone ($\sim 830 \mu\text{J}$). As illustrated in Fig. 4(b), however, the two and three component alkali-rare gas mixtures exhibit laser thresholds with respect to the *absorbed* pump pulse energy that are, to within experimental uncertainty, identical.

Several conclusions can be drawn from Figs. 3 and 4. Although Cs–Ar–Kr mixtures reduce the D_2 laser pump energy threshold significantly (relative to that for the binary Cs–Ar mixture), the partial substitution of Kr for Ar has no discernible effect on the laser excitation spectral profile. It is evident, therefore, that Kr assists the photoassociation of Cs–Ar pairs because it is the Cs–Ar interaction potentials that dominate the excitation spectrum. These considerations suggest that three body photoassociation of Cs–Ar–Kr atomic ensembles has been observed and is responsible for reducing the pump energy threshold by $>25\%$.

In summary, lasing on the 852.1 nm (D_2) transition of Cs has been observed when Cs–Ar and Cs–Ar–Kr mixtures are photoexcited through the blue satellite of the transition. Lasing at this wavelength is not an option with previous three level laser schemes based upon pumping the atomic species directly, and the quantum efficiency for this four level system is $>98\%$. Comparisons of laser excitation spectra and output pulse energy data for Cs–Ar and Cs–Ar–Kr mixtures suggest that three body photoassociation of the Cs–Ar–Kr collision complex has been observed and this process is effective in accessing the Cs ($^2\text{P}_{3/2}$) upper laser level. The introduction of Kr to the laser mixture does not influence noticeably the laser excitation spectrum, indicating that Kr increases the

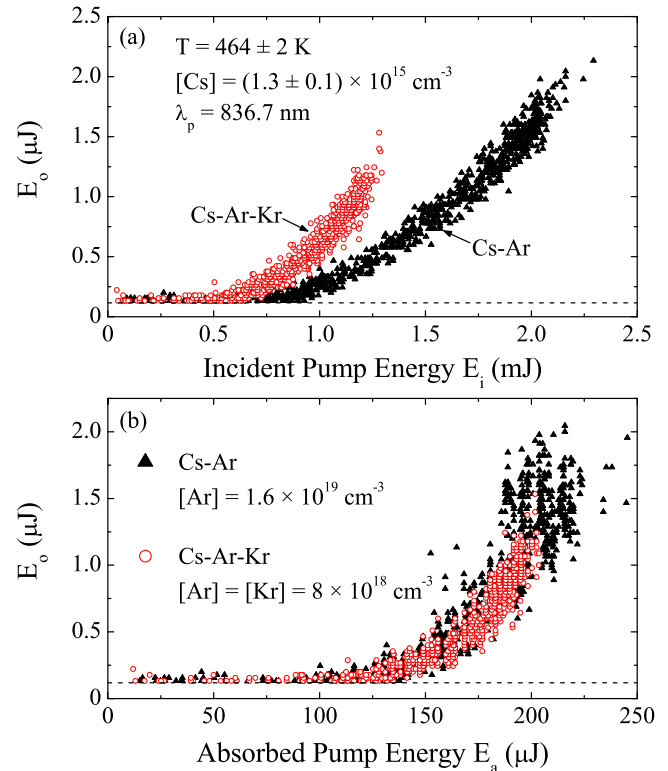


FIG. 4. (Color online) D_2 laser output pulse energy (E_o) measurements: (a) Comparison of Cs–Ar and Cs–Ar–Kr mixtures for which the abscissa indicates the incident pulse energy E_i ; (b) the same data as (a) but presented as a function of the absorbed pulse energy (E_a). The temperature was maintained at $464 \pm 2 \text{ K}$ for all measurements, and the Ar and Kr number densities are both $8 \times 10^{18} \text{ cm}^{-3}$ for the Cs–Ar–Kr experiments. In obtaining the Cs–Ar data, $[\text{Ar}]$ was fixed at $1.6 \times 10^{19} \text{ cm}^{-3}$, and the dashed horizontal lines in (a) and (b) reflect the detection limit for the pyroelectric detectors.

reduced absorption coefficient at the pump wavelength by $\sim 5\text{--}10\%$ but plays a role subordinate to Ar with respect to the interaction potentials shaping the excitation spectrum.

The technical assistance of C. J. Wagner, T. M. Spinka, and the support of the U.S. Air Force Office of Scientific Research under Contract No. FA9550-07-1-0575 and Grant Nos. FA9550-07-1-0003 and FA9550-10-1-0048 are gratefully acknowledged.

¹W. F. Krupke, R. J. Beach, V. K. Kanz, and S. A. Payne, *Opt. Lett.* **28**, 2336 (2003).

²R. J. Beach, W. F. Krupke, V. K. Kanz, S. A. Payne, M. A. Dubinskii, and L. D. Merkle, *J. Opt. Soc. Am. B* **21**, 2151 (2004).

³B. Zhdanov, C. Maes, T. Ehrenreich, A. Havko, N. Koval, T. Meeker, B. Worker, B. Flusche, and R. J. Knize, *Opt. Commun.* **270**, 353 (2007).

⁴J. D. Readle, C. J. Wagner, J. T. Verdeyen, D. L. Carroll, and J. G. Eden, *Electron. Lett.* **44**, 1466 (2008).

⁵J. D. Readle, C. J. Wagner, J. T. Verdeyen, T. M. Spinka, D. L. Carroll, and J. G. Eden, *Appl. Phys. Lett.* **94**, 251112 (2009).

⁶J. D. Readle, J. T. Verdeyen, J. G. Eden, S. J. Davis, K. L. Galbally-Kinney, W. T. Rawlins, and W. J. Kessler, *Opt. Lett.* **34**, 3638 (2009).

⁷S. Chilukuri, *Appl. Phys. Lett.* **34**, 284 (1979).

⁸S. N. Atamas, L. M. Bukshpun, Yu. V. Koptev, E. L. Latush, and M. F. Sém, *Kvantovaya Elektron. (Moscow)* **11**, 229 (1984) [*Sov. J. Quantum Electron.* **14**, 161 (1984)].